Evidence for Multiple Substrate-Reduction Sites and Distinct Inhibitor-Binding Sites from an Altered *Azotobacter vinelandii* Nitrogenase MoFe Protein†

Joan Shen,‡ Dennis R. Dean, and William E. Newton*

Department of Biochemistry, Virginia Polytechnic Institute and State University, Blacksburg, Virginia 24061-0308

Received November 19, 1996; Revised Manuscript Received January 29, 1997⊗

ABSTRACT: The arginine-277 residue of the α-subunit of the nitrogenase MoFe protein was targeted for substitution because it is (i) a close neighbor of α-cysteine-275, which is one of only two residues anchoring the FeMo cofactor to the polypeptide, and (ii) a component of a potential channel for entry/exit of substrates/products and for accepting FeMo cofactor during MoFe-protein maturation. Several of the eight mutant strains constructed were capable of good diazotrophic growth and also contained FeMo cofactor as indicated by its biologically unique $S = 3/2$ EPR spectrum. These observations indicate that the positively charged α-arginine-277 residue is not required for acceptance of the negatively charged FeMo cofactor by the separately synthesized, cofactor-deficient, apo-MoFe protein. The wide range of nitrogen-fixation phenotypes shown by these mutant strains generally correlated well with their C_2H_2- and proton-reduction activities, which range from 5 to 65% of wild-type activity. One notable exception is the histidine-substituted strain, DJ788 (α-277^{His}). This strain, although unable to fix N_2 and grow diazotrophically, elaborates an altered α-277^{His} MoFe protein that catalyzes the reduction of the alternative substrates, C_2H_2, HCN, HN_3, and protons. These observations are best explained if multiple redox levels are available to the MoFe protein but the α-277^{His} MoFe protein is incapable of reaching the more-reduced redox levels required for nitrogen fixation. Under nonsaturating CO concentrations, the α-277^{His} MoFe-protein-catalyzed reduction of C_2H_2 showed sigmoidal kinetics, which is consistent with inhibitor-induced cooperativity among two C_2H_4-evolving sites and indicates the presence of three sites, which can be simultaneously occupied, on the MoFe protein. Similar kinetics were not observed for α-277^{His} MoFe-protein-catalyzed reduction of either HCN or HN_3 with nonsaturating CO levels, indicating that these substrates are unlikely to share common binding sites with C_2H_2. Further, CN^- did not induce cooperativity in C_2H_2 reduction and, therefore, CO and CN^- are unlikely to share a common binding site. These changed substrate specificities, reinforced by changes in the FeMo-cofactor-derived $S = 3/2$ EPR spectrum, clearly indicate the importance of the α-277 residue in catalysis and the delicate control exerted on the properties of bound FeMo cofactor by its polypeptide environment.

The two component proteins of nitrogenase, the Fe protein[1] and MoFe protein, together catalyze the MgATP-dependent reduction of dinitrogen (N_2), protons, and a variety of other small-molecule substrates. The Fe protein is a homodimer that contains a [4Fe-4S] cluster bridged between its identical subunits. It also contains nucleotide-binding sites and serves as an obligate electron donor to the MoFe protein. The MoFe protein is an $\alpha_2\beta_2$ heterotetramer and it provides the substrate-binding and -reduction sites. Each α-β pair within the MoFe protein is believed to operate as an independent catalytic unit. Substrate reduction is accomplished through the sequential association and dissociation of the two component proteins in a process coupled to nucleotide hydrolysis and a series of one-electron transfers from the Fe protein to the MoFe protein (Silverstein & Bulen, 1970; Davis *et al.*, 1975; Hageman & Burris, 1978; Lowe & Thorneley, 1984). Under optimal catalytic conditions, one electron is transferred and two molecules of MgATP are hydrolyzed for each association−dissociation event. Although electrons are transferred to the MoFe protein only one-at-a-time, at least two electrons and as many as eight electrons are required for the reduction of any nitrogenase substrate. Thus, nitrogenase catalysis requires the accumulation of multiple electrons within the MoFe protein. How these electrons are accumulated and distributed within the MoFe protein is not known. It is generally believed that a unique metallocluster, called the P cluster, is involved in accepting electrons from the Fe protein and mediating their subsequent intramolecular delivery to the substrate-reduction site (Dean *et al.*, 1990; Lowe *et al.*, 1993; Peters *et al.*, 1995a). There are two P clusters in the MoFe-protein heterotetramer, and each is comprised of two [4Fe-4S] subclusters that bridge an α-β unit interface (Kim & Rees, 1992a,b, 1994; Chan *et al.*, 1993; Bolin *et al.*, 1993a,b). The substrate-reduction site on the MoFe protein is provided by

† Supported by the National Institutes of Health (Grant DK-37255).

* To whom correspondence should be addressed (tel., 540-231-6315; fax, 540-231-9070; email, wenewton@vt.edu).

‡ Present address: Department of Microbiology, University of California at Los Angeles, Los Angeles, CA 90095.

⊗ Abstract published in *Advance ACS Abstracts,* April 1, 1997.

[1] Abbreviations: MoFe protein, the larger molybdenum- and iron-containing protein component of nitrogenase (also known as component 1); Fe protein, the smaller iron-containing protein component of nitrogenase (also known as component 2); FeMo cofactor, the molybdenum- and iron-containing prosthetic group of the MoFe protein; P cluster, the 8Fe-containing prosthetic group of the MoFe protein; MgATP, the magnesium salt of adenosine triphosphate; Tris, tris(hydroxymethyl)aminomethane; Hepes, *N*-(2-hydroxyethyl)piperazine-*N*′-2-ethanesulfonic acid; Tes, *N*-[tris(hydroxymethyl)methyl]-2-aminoethanesulfonic acid; BCA, bicinchoninic acid; SDS, sodium dodecyl sulfate; EPR, electron paramagnetic resonance; Nif, nitrogen fixation.

S0006-2960(96)02857-7 CCC: $14.00

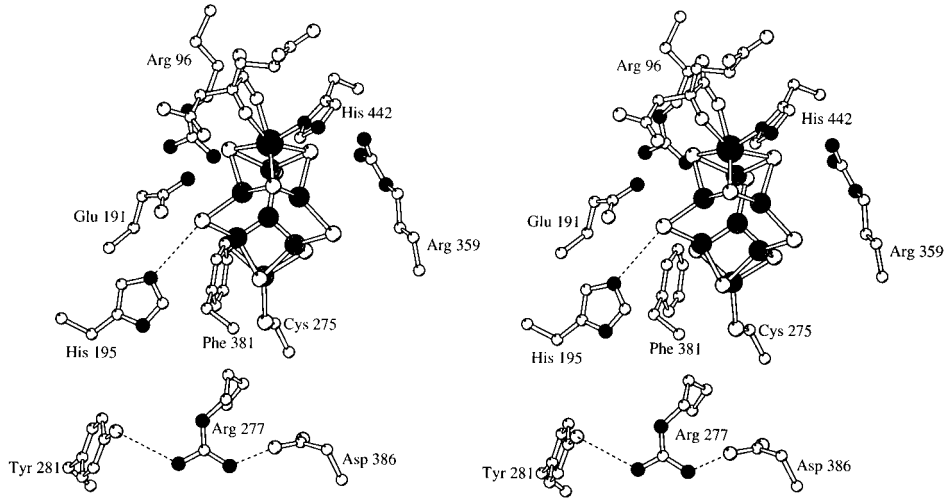

FIGURE 1: Stereoscopic view of the FeMo cofactor and its surrounding environment. In the upper part of the figure, the Mo atom of FeMo cofactor is ligated by the α-histidine-442 residue and a molecule of homocitrate. The lower part of the figure shows ligation of a unique Fe atom by α-cysteine-275 and the hydrogen-bonding interactions of its close neighbor, α-arginine-277. The largest and darkest sphere is the Mo atom, the spheres of intermediate size and shading are the Fe atoms, and the smallest and lightest-shaded spheres are S atoms. In the protein and homocitrate components, the C atoms are unshaded, whereas the N atoms are shaded darker than the O atoms. The figure was prepared using the MOLSCRIPT program (Kraulis, 1991).

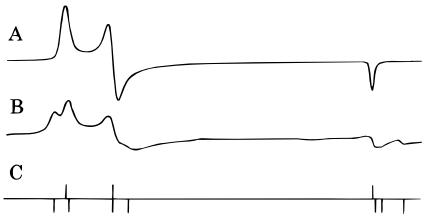

FIGURE 2: EPR spectra of purified wild-type (A) and α-277^{His} (B) MoFe proteins. Spectra were recorded at a microwave frequency of 9.22 GHz and a microwave power of 20 mW with a 100-kHz field modulation of 25 G at 12 K. Both protein samples were ca. 25 mg/mL in 25 mM Tris-HCl, pH 7.4, containing 25 mM NaCl and 2 mM $Na_2S_2O_4$. Panel C is a stick diagram of both spectra to show the relative apparent *g* values of 4.32, 3.65, and 2.01 for wild-type (above the line) and 4.52, 4.25, 3.63, 3.48, 1.99, and 1.90 for the α-277^{His} MoFe protein (below the line). A third line around $g = 2$ (observable at 1.97) in the latter spectrum suggests a third overlapping $S = 3/2$ spectrum.

a second metallocluster prosthetic group, called the FeMo cofactor (Shah & Brill, 1977; Hawkes *et al.*, 1984; Scott *et al.*, 1990, 1992; Kim *et al.*, 1995). Each MoFe-protein α-subunit carries one FeMo-cofactor molecule. FeMo cofactor is composed of a [4Fe-3S] subcluster and a [Mo-3Fe-3S] subcluster that are connected by three bridging inorganic sulfides (Figure 1; Kim & Rees, 1992a,b; Chan *et al.*, 1993; Bolin *et al.*, 1993a,b). Homocitrate is an organic constituent of FeMo cofactor and it is coordinated to the Mo atom through its 2-hydroxyl and 2-carboxyl groups. In its native state, the MoFe protein exhibits a biologically unique $S = 3/2$ electron paramagnetic resonance (EPR) signal that arises from FeMo cofactor.

In the presence of MgATP, a suitable source of reducing equivalents and an anaerobic environment, Mo-nitrogenase catalyzes the reduction of a variety of small molecule substrates in addition to N_2. Among these alternative substrates are protons (Burns & Bulen, 1965), acetylene (Dilworth, 1966), azide (both HN_3 and N_3^- are substrates; Rubinson *et al.*, 1985), and cyanide (HCN is a substrate, but CN^- is an inhibitor of total electron flux; Li *et al.*, 1982). In fact, the complexity of nitrogenase catalysis can be appreciated not only from the structures, organization, and interactions of the metalloclusters associated with electron transfer and substrate binding but also from the nature and relationships among the many nitrogenase substrates and inhibitors. Indeed, the interactions among various substrates have proven to be very complicated (Hwang & Burris, 1972; Hwang *et al.*, 1973; Rivera-Ortiz & Burris, 1975; Davis *et al.*, 1975; Dilworth & Thorneley, 1981; Li *et al.*, 1982; Rubinson *et al.*, 1985). The effect of carbon monoxide (CO) on catalysis presents yet another complexity because it is a noncompetitive inhibitor of the reduction of all nitrogenase substrates except protons (Hardy *et al.*, 1965; Bulen *et al.*, 1965). Its presence diverts all electrons to proton reduction with no effect (or possibly a slight increase) on the total electron flux through the enzyme regardless of either the presence or concentration of other potential substrates. CO also elicits two distinct EPR signals from nitrogenase during turnover; one under low and the other under high concentrations of CO (Davis *et al.*, 1979). The appearance of neither signal, however, correlates with the onset of CO inhibition of substrate reduction, which suggests multiple CO-binding sites on the enzyme complex.

Attempts to explain these apparently contradictory observations have postulated the presence of both multiple-binding sites and multiple redox levels on the enzyme. Thus, the different substrates and inhibitors may bind to the enzyme either at different sites or at different redox levels of the same site. Redox level-dependent substrate binding and reduction is an important consideration of the Lowe and Thorneley (1984) kinetic model of nitrogenase catalysis. In this model, each sequential step in the transfer of single electrons from the Fe protein to the MoFe protein leads progressively to a MoFe protein at an increasingly reduced level, labeled as E_0, E_1, E_2, etc. These different redox levels of the MoFe protein are proposed to bind the various substrates selectively. For example, N_2 is proposed to bind to states E_3 and E_4, i.e., only after three or four electrons have been accepted, whereas protons can be reduced to H_2 at the less-reduced state of E_2. This model explains why protons rather than N_2 are preferentially reduced under conditions of low electron flux, where the state E_2 will prefer

to evolve H_2 and revert to the E_0 state, rather than to progress to E_3 and bind N_2. In contrast, C_2H_2 is proposed to bind reversibly to species E_1 and E_2 of the MoFe protein, which are also involved in H_2 formation. This possibility is consistent with C_2H_2 being a more effective competitor of H_2 evolution than is N_2 (Lowe *et al.*, 1990). Finally, the fact that N_2 must bind at a more reduced level than does C_2H_2 also explains the observed nonreciprocity of kinetic patterns when both are present.

One approach to deciphering the nature of the interactions among various substrates and inhibitors and to test the Lowe−Thorneley model is to alter the FeMo-cofactor environment through targeted amino-acid substitution and to monitor its effects on the catalytic and spectroscopic properties of the resulting altered MoFe protein (Scott *et al.*, 1990; Newton & Dean, 1993). The recent availability of a three-dimensional model of the MoFe protein (Kim & Rees, 1992a,b, 1994; Chan *et al.*, 1993; Kim *et al.*, 1993; Bolin *et al.*, 1993a,b) now affords the rational basis for the design and interpretation of such amino-acid-substitution studies. The feasibility of this approach was demonstrated previously (Scott *et al.*, 1990, 1992; Kim *et al.*, 1995; DeRose *et al.*, 1995). In the present study, the α-arginine-277 residue was targeted because it is in a region of the α-subunit polypeptide that includes α-cysteine-275, which provides a mercaptide ligand to FeMo cofactor (Brigle *et al.*, 1985; Kent, *et al.*, 1989; Kim & Rees, 1992a). Further, the crystallographic model has revealed that α-arginine-277, together with α-serine-192 and α-glycine-356, might be involved in providing the entry/exit route for substrates and products as well as being a component of a channel for FeMo-cofactor insertion during biosynthesis of the MoFe protein (Kim & Rees, 1992b).

In this report, we (i) compare the characteristics of eight *Azotobacter vinelandii* mutants, each having a single amino-acid substitution at α-arginine-277 of the MoFe protein at the whole-cell and crude extract levels, with those from wild-type; (ii) use spectroscopic methods to detect changes in the FeMo-cofactor environment due to the substitutions; and (iii) analyze the N_2-, proton-, C_2H_2-, HCN-, and HN_3-reduction properties of the altered α-277^{His} MoFe protein purified from mutant strain DJ788 for comparison with those of the wild-type enzyme isolated from strain DJ527. These probes constitute a continuation of our efforts to unravel the complexity of nitrogenase catalysis at the molecular level.

EXPERIMENTAL PROCEDURES

Mutant Strain Construction. Methods for degenerate oligonucleotide synthesis and use, site-directed mutagenesis, gene replacement, and the isolation of mutant strains were performed as described or cited previously (Brigle *et al.*, 1987a, b; Kim *et al.*, 1995). Each altered MoFe protein is designated by the name of the subunit (α in this case), the number of the amino-acid position substituted, followed by the three-letter code for the substituting amino acid in superscript form, *e.g.*, the altered MoFe protein having the α-arginine-277 residue substituted by threonine is designated as α-277^{Thr}. Strains are designated by DJ numbers. DJ527 is a strain harboring an insertion mutation within *hox*KG, which abolishes its uptake hydrogenase activity, but retains all of its *nif* genes intact (Kim *et al.*, 1995). All mutants used in this study are derived from DJ527 and exhibit a Hup^- phenotype, which enables H_2-evolution activity to be measured at the crude extract level without interference from endogenous uptake hydrogenase activity.

Growth Conditions, Media, and Nitrogenase Derepression. Small batches of *A. vinelandii* wild-type and mutant strains were grown at 30 °C in Fernbach flasks on a modified Burk medium (Strandberg & Wilson, 1968) containing 10 μM Na_2MoO_4, which is sufficient to repress the alternative nitrogenase systems, plus 20 mM filter-sterilized urea. Cultures were grown under air with shaking at 250 rpm. Larger-scale *Azotobacter* cultures were grown in a 28-L fermentor (New Brunswick Scientific Company, New Brunswick, NJ) on the modified Burk medium, plus Na_2MoO_4 and urea as described above, with an air-flow rate of 35−40 L min^{-1} and vigorous stirring of 250 rpm. Cell growth was monitored using a Klett−Summerson meter (Klett Mfg. Co. Inc., New York) equipped with a no. 54 filter until the cell density reached ca. 150 Klett units. The cultures were then derepressed for nitrogenase synthesis (Jacobson *et al.*, 1989). *A. vinelandii* cells were harvested and stored at −80 °C until used.

Crude Extract Preparation. Cells were thawed and diluted anaerobically at 4 °C in degassed 50 mM Tris-HCl (pH 8.0), containing 2 mM sodium dithionite, at the approximate ratio of 1.0 g of cells to 2.0 mL of buffer. For smaller-scale preparations, the cell suspension was broken with 3-min pulse sonication using a Heat System Sonicator model XL2015 in a 25-mL Rosette cooling cell (Heat Systems-Ultrasonics, Inc.) immersed in an ice−water bath to offset increasing temperature. When larger-scale isolations were undertaken, the cells were diluted similarly but cell rupture was accomplished using a Manton−Gaulin homogenizer. In both cases, the resulting extract was transferred anaerobically into centrifuge tubes and centrifuged at 4 °C for 60 min at 98000*g*. The supernatant was frozen and stored in liquid nitrogen until used.

MoFe-Protein Purification. The altered α-277^{His} MoFe protein of the mutant strain DJ788 and the wild-type (α-277^{Arg}) MoFe protein from strain DJ527 were purified in parallel. Cells of both strains were grown up individually using a 28-L fermentor (see Growth Conditions, Media, and Nitrogenase Depression above). Crude extract was prepared as above, heat-treated at 56 °C for 5 min, before centrifugation at 98000*g* at 4 °C for 1 h to separate the cell debris, which was discarded. Partial purification of the MoFe protein was achieved by chromatography over DE52-cellulose (Whatman Biosystems Ltd, England), followed by a Q-sepharose column (Pharmacia LKB, Sweden), both of which were anaerobically equilibrated with 25 mM Tris-HCl (pH 7.4), containing 1 mM sodium dithionite. On both columns, a linear NaCl gradient from 0.1 to 1.0 M in degassed 25 mM Tris-HCl (pH 7.4), 1 mM sodium dithionite, was applied and both MoFe proteins eluted at ca. 0.2 M NaCl off the DE52-cellulose column and at ca. 0.35 M NaCl off the Q-sepharose column. This protocol resulted in about 70% recovery of MoFe-protein activity devoid of Fe-protein activity. Further purification of the MoFe proteins was achieved by Sephacryl S-300 gel filtration (Pharmacia LKB, Sweden) chromatography using degassed 0.2 M NaCl in 25 mM Tris-HCl (pH 7.4), 1 mM sodium dithionite, to yield pure samples of both MoFe proteins (see Table 2). The wild-type Fe protein used in the assays was purified from *A. vinelandii* wild-type as described previously (Burgess *et al.*,

Table 1: Nif Phenotypes, Diazotrophic Growth Rates, and Crude Extract MoFe Protein and Fe Protein Specific Activities of α-277 Mutant Strains

strain[a]	substitution at α-277	codon	DT[b] (h)	under 10% C_2H_2[c] C_2H_4	under 10% C_2H_2[c] H_2	under Ar[d] MoFe, H_2	under Ar[d] Fe, H_2
DJ527	none (Arg)	CGC	2.0	78	6.4	78	40
DJ974	Lys	AAG	3.2	20	3.7	27	21
DJ679	Cys	TGC	4.0	51	2.6	51	30
DJ681	Thr	ACC	5.0	37	7.5	46	36
DJ978	Phe	TTC	6.0	21	5.3	32	34
DJ976	Leu	CTC	12.7	15	3.9	20	34
DJ788	His	CAC	N/G	27	16	46	37
DJ745	Gly	GGC	N/G	3.5	0.6	3.7	29
DJ747	Pro	CCT	N/G	5.8	0.1	4.0	19

[a] All strains are deleted for the uptake hydrogenase structural genes resulting in Hup^- phenotype. [b] DT denotes the doubling time of the corresponding *Azotobacter* strain grown in air on nitrogen-free Burk medium. N/G indicates no growth under these conditions. [c] MoFe protein specific activity in the crude extract is listed as nanomoles of C_2H_4 and H_2 produced per minute per milligram of total protein under a 10% C_2H_2/90% Ar atmosphere in the presence of optimal amount of purified Fe protein. [d] MoFe protein and Fe protein specific activities in the crude extract are listed as nanomoles of H_2 produced per minute per milligram of total protein under a 100% Ar atmosphere. All assays were performed with optimal amount of purified complementary protein present.

Table 2: Purification Table for the DJ527 (α-277^{Arg}) and DJ788 (α-277^{His}) MoFe Proteins

step[a]	total protein[b] WT[e]	total protein[b] RH[e]	total activity[c] WT	total activity[c] RH	specific activity[d] WT	specific activity[d] RH	fold purified WT	fold purified RH	yield (%) WT	yield (%) RH
CE	12.0	13.0	1.26	0.75	105	58	1	1	100	100
DE-52	1.80	2.00	0.98	0.58	545	290	5	5	78	77
Q-seph	0.89	1.15	0.87	0.52	980	450	9	8	69	69
S-300	0.26	0.34	0.64	0.33	2450	980	23	17	51	44

[a] Crude extracts were obtained using a Manton−Gaulin homogenizer for cell rupture, followed by heat treatment at 56 °C for 5 min, and centrifugation at 98000*g* for 1 h; DE-52 represents the product of chromatography over the weak anion exchanger, DE-52 cellulose; Q-seph is the product after the strong anion exchanger, Q-sepharose; S-300 represents the product after the gel-filtration resin, Sephacryl S-300. [b] Expressed in units of grams. [c] Expressed as H_2 evolved in units of millimoles per minute. [d] Expressed as H_2 evolved in units of nanomoles per minute per milligram. [e] RH and WT represent the α-277^{His} and wild-type MoFe proteins, respectively.

1980) and had a specific activity of 2060 nmol of H_2 (min mg)$^{-1}$.

Protein Estimation and Gel Electrophoresis. The BCA method was used for protein estimation with bovine serum albumin as a standard (Smith *et al.*, 1985). For SDS−PAGE, samples and gels were prepared according to Laemmli (1970). The gels used were 12% polyacrylamide (1.35% cross-linker) with a 4% stacking gel. Electrophoresis was performed at 30 mA/gel in a Hoefer Mighty Small apparatus (Hoefer, San Francisco, CA), using 10000−100000 low molecular weight standards (Biorad Laboratories, Hercules, CA) and the gels stained with Coomassie Blue (R-250).

Metal Analysis. The molybdenum and iron content of purified α-277^{His} and wild-type MoFe proteins were determined using a Perkin-Elmer Plasma 400 Emission Spectrometer.

Nitrogenase Activity Assay. MoFe-protein and Fe-protein specific activities were measured in both crude extracts and purified proteins in the presence of an optimal amount of the purified complementary component protein as described previously (Kim *et al.*, 1995). All assays were terminated by addition of 0.25 mL of 0.5 M Na_2EDTA (pH 7.5) after 8 min using a syringe. With the purified proteins, a total of 0.5 mg of nitrogenase proteins in 1 mL was used to avoid complications introduced by both high- and low-protein concentrations at a constant Fe-protein:MoFe-protein molar ratio of 20:1, *i.e.*, under high-flux conditions. When required, CO was added by gas-tight Hamilton syringe (Hamilton Syringe Co., Reno, NV) to the appropriate assay vial during the preincubation period. Each assay series was independently run at least three times with individual data points measured in triplicate. The data points plotted in Figures 3 and 4 are the averages of the triplicate assays.

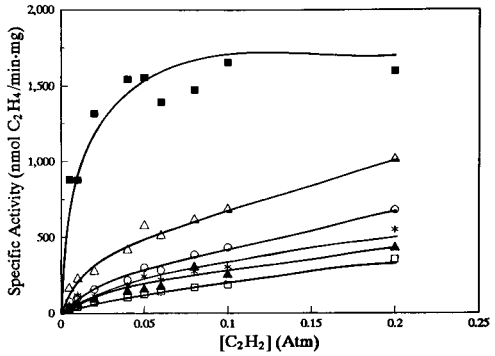

FIGURE 3: Michaelis−Menten plots of C_2H_2 reduction catalyzed by wild-type MoFe protein in the absence and presence of CO. Amount of CO present in the C_2H_2-reduction reactions is represented by ■ (no CO); △ (6.25×10^{-4} atm CO); ○ (1.25×10^{-3} atm CO); * (1.9×10^{-3} atm CO); ▲ (2.5×10^{-3} atm CO); □ (3.1×10^{-3} atm CO).

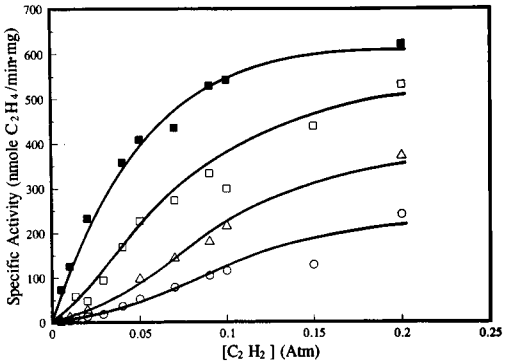

FIGURE 4: Michaelis−Menten plots of C_2H_2 reduction catalyzed by the α-277^{His} MoFe protein in the absence and presence of CO. Amount of CO used is represented by: ■ (no CO); □ (2.5×10^{-4} atm CO); △ (6.25×10^{-4} atm CO); ○ (1.25×10^{-3} atm CO).

Substrate Preparations. All reaction vials were subject to four cycles of evacuation and flushing using an automated machine (Corbin, 1978) to replace the air with either 100% Ar or 100% N_2, depending on the type of assay to be conducted. In catalyzed C_2H_2-reduction assays, dilution of a 100% Ar atmosphere with aliquots of C_2H_2 produced from the reaction of calcium carbide (Fisher Scientific, Pittsburgh, PA) with water was used to produce the desired C_2H_2 concentration in each reaction vial. Catalyzed H^+-reduction assays were performed under a 100% Ar gas phase. For the assays involving HN_3 reduction, appropriate aliquots of a 100-mM NaN_3 in 25 mM Hepes-KOH (pH 7.4) stock solution were added to each reaction vial before the atmosphere-replacement step. The HN_3 concentration is calculated as 1.582×10^{-3} [NaN_3] at pH 7.4 (Rubinson *et*

al., 1985). For the assays involving HCN reduction, a known amount of a pH-adjusted, 100-mM, degassed NaCN in 25 mM Hepes-KOH (pH 7.4) stock solution was injected into each reaction vial during the preincubation period. HCN is the substrate in NaCN-based assays (Li *et al.*, 1982), and its concentration can be calculated at pH 7.4 using the formula [HCN] = 0.981[NaCN].

Product Analysis. C_2H_4 and CH_4 were quantified by gas chromatography on a Poropak N column using a flame ionization detector (Shimadzu, Tokyo, Japan). H_2 production was quantified by gas chromatography on a molecular sieve 5A column and a thermal conductivity detector (Shimadzu, Tokyo, Japan). Calibrations were performed using standard gases of 1 ppm C_2H_4 in helium, 1 ppm CH_4 in helium, and 1% H_2 in N_2 (Scotty Specialty Gases, Plumsteadville, PA), respectively. Ammonia production was measured by the phenol/hypochlorite colorimetry method (Dilworth *et al.*, 1992). Hydrazine (N_2H_4) production in the azide-reduction assays was measured using the *p*-dimethylaminobenzaldehyde colorimetric assay method (Dilworth & Thorneley, 1981).

Buffers Used in the Studies. Purified MoFe proteins were dialyzed into 25 mM Tes-KOH (pH 7.4) for all assays except those involving NH_3 determinations, which used 25 mM Hepes-KOH (pH 7.4) to minimize inhibition of color development (Dilworth *et al.*, 1992).

EPR Spectroscopy. Derepressed whole cells were prepared for EPR spectroscopy as described previously (Scott *et al.*, 1990). The spectra of both whole cells and purified MoFe proteins were recorded on a Varian Associates E-line instrument at a microwave frequency of 9.22 GHz and a microwave power of 20 mW with a 100-kHz field modulation of 25 G at 12 K maintained by liquid helium boil-off.

RESULTS

Characteristics of Diazotrophic Growth and Nitrogenase Catalytic Activities in Crude Extracts. Eight mutant strains, each having a specific amino-acid substitution for residue α-arginine-277 in the MoFe protein of *A. vinelandii*, were produced using site-directed mutagenesis and gene-replacement methods (Brigle *et al.*, 1987a; Jacobson *et al.*, 1989). Table 1 summarizes the MoFe-protein and Fe-protein specific activities for crude extracts prepared from nitrogenase-derepressed wild-type and mutant strains along with their diazotrophic-growth behavior. These mutant strains show a wide range of Nif phenotypes, from Nif^+ through Nif^{slow} to Nif^-. The crude extracts prepared from all mutant strains have lower C_2H_2- and proton-reduction activities, ranging from ca. 5 to 65% of wild-type activity. These activities generally correlate well with the corresponding growth rates except that the histidine-, proline-, and glycine-substituted strains are strictly Nif^-, but all three retain some C_2H_2- and proton-reducing activity. The comparisons of activities in crude extracts are meaningful because each extract has approximately the same amount of nitrogenase polypeptides as measured by both SDS-PAGE analysis and by their respective levels of Fe-protein activity. For all strains, crude extract assays, performed under high-flux conditions and in the presence of 10% CO, resulted in the complete inhibition of C_2H_2 reduction with all electron flux being directed to proton reduction.

The most remarkable biochemical phenotype was exhibited by the mutant strain DJ788 (α-277^{His}). Even though this strain is unable to grow diazotrophically, it exhibits MoFe-protein C_2H_2- and proton-reduction activities that are approximately 45% of the wild-type rates. In addition, its approximately 2:1 distribution of electrons among C_2H_4 and H_2 production, when assayed under a 10% C_2H_2/90% Ar atmosphere, is very different to the approximately 10:1 electron allocation exhibited by wild-type. Unlike some altered MoFe proteins (Scott *et al.*, 1990, 1992; Kim *et al.*, 1995), no C_2H_6 was detected from any crude extract prepared in this study when assayed under C_2H_2.

Whole-Cell EPR Spectra. All of the altered MoFe proteins displayed variously changed EPR signals in the $g = 4$ region when examined in whole-cell preparations. Although there was no change in line width, line shape, or intensity in the whole-cell EPR spectrum of DJ974 (α-277^{Lys}), it did exhibit a very minor rhombic shift to $g = 4.35$ and 3.63 when compared to the wild-type values of $g = 4.34$ and 3.65. The whole-cell EPR spectrum of DJ679 (α-277^{Cys}) cells also had EPR intensity comparable to that of wild-type but showed a slight axial distortion ($g = 4.30$ and 3.72). Substitutions by either leucine or phenylalanine resulted in both a slight broadening and a small increase in the rhombicity of their respective whole-cell EPR spectra when compared to wild-type. Both substitutions caused diminished EPR intensity, 25 and 40% of wild-type intensity, respectively, in line with their slower diazotrophic growth rates. Strains DJ745 (α-277^{Gly}) and DJ747 (α-277^{Pro}), which are unable to grow diazotrophically, exhibited only very weak EPR signal intensities (<10% of wild-type).

In contrast to the other strains, the whole-cell EPR spectra from DJ788 (α-277^{His}) and DJ681 (α-277^{Thr}) are dramatically altered. Both substitutions result in the appearance of more than the two EPR lines expected in the $g = 4$ region. Both EPR spectra have intensities comparable to that of wild-type. The EPR spectrum elicited from DJ681 cells has two resonances at $g = 3.76$ and 3.56, but three lines at $g = 4.50$, 4.30, and 4.03. Although the $g = 4.50$ line should pair with $g = 3.56$ line, it is not certain which of the 4.30/4.03 lines pairs with the $g = 3.76$ line. However, the occurrence of three lines above $g = 4$ indicates that three overlapping $S = 3/2$ spectra exist in strain DJ681. For DJ788 (α-277^{His}) cells, two sets of signals are observed; the major pair of resonances at $g = 4.25$ and 3.63, which are close to wild-type values, account for ca. 80% of the signal intensity, and the minor rhombically distorted pair at $g = 4.52$ and 3.48 account for the remaining ca. 20% of the intensity. These multiple sets of EPR signals (see Figure 2) may indicate either that FeMo cofactor is bound in two (or more) major orientations within its polypeptide pocket (and possibly oscillating among them) or they may represent FeMo-cofactor intermediates that occur during turnover but are not usually observed in the steady state. There is no obvious correlation of the intensities of the two signal sets, 2:1 for DJ681 and 4:1 for DJ788, with any observed catalytic property, so discrete aspects of catalysis cannot be specifically assigned to either of the EPR observable species.

The observed EPR intensities (except possibly for those with the leucine, proline, or glycine substitution), which range from about 50 to 100% of the intensity of wild-type, are consistent with a full complement of protein-bound FeMo cofactor. These intensities also correlate quite well with both the diazotrophic growth rate and the C_2H_2- and H^+-reducing activities of the respective MoFe proteins.

Purification of the Altered MoFe Protein from DJ788. The purification of MoFe proteins from both DJ788 (α-277^{His}) and wild-type (α-277^{Arg}) strains was performed in parallel to minimize any variation potentially introduced by different purification protocols (Table 2). Similar levels of purification were achieved for both proteins as judged by their activities and migration pattern on SDS−PAGE (data not shown). At all stages of purification, the α-277^{His} MoFe protein exhibits about 45% of the activity of wild-type. After Sephacryl S-300 gel filtration, the two proteins have specific activities of 980 and 2450 nmol of H_2 (min mg of protein)$^{-1}$, respectively. In addition, under a 10% C_2H_2/90% Ar atmosphere, the altered α-277^{His} MoFe protein allocated approximately 35% of total electron flux to H_2 evolution, the same distribution as found for the corresponding crude extract. The EPR spectrum of purified α-277^{His} MoFe protein also retained the same line shapes and g values in the $g = 4$ region as were observed in the whole-cell spectrum, plus the intensities of the major and minor set of FeMo-cofactor resonances remained at a 4:1 proportion (Figure 2). These data establish that the changed catalytic properties of the purified α-277^{His} MoFe protein are a direct result of the introduced substitution *per se* rather than as a consequence of the purification protocol. Metal analysis of the purified α-277^{His} MoFe protein gave 1.3 Mo atoms per $\alpha_2\beta_2$ tetramer with a Fe:Mo ratio of 15:1, which compares with the values of 1.8 Mo atoms per $\alpha_2\beta_2$ tetramer and a 15:1 Fe:Mo ratio consistently measured for the wild-type. The Mo content of the α-277^{His} MoFe protein is consistent with its EPR spectral intensity, which is also about 70% of that of wild-type.

The α-277^{His} MoFe Protein neither Binds nor Reduces N_2. When the α-277^{His} MoFe protein was assayed under a 100% N_2 under high-flux conditions, neither NH_3 nor N_2H_4 was produced. The latter was also not detectable as an intermediate using an acid-quenched reaction assay under 100% N_2 (Thorneley *et al.*, 1978). Similarly, no nitrogenous product was detected when the α-277^{His} MoFe protein was assayed with hydrazine as a substrate. In addition, the proton-reduction activity catalyzed by the α-277^{His} MoFe protein was the same when assayed under either a 100% Ar atmosphere or a 100% N_2 atmosphere. Finally, the pattern of H_2 and C_2H_4 production catalyzed by the α-277^{His} MoFe protein was the same under either a 10% C_2H_2/90% Ar atmosphere or a 10% C_2H_2/90% N_2 atmosphere. Thus, unlike the normal MoFe protein (Rivera-Ortiz & Burris, 1975), N_2 is not an inhibitor of the α-277^{His} MoFe-protein-catalyzed reduction of either protons or C_2H_2. This conclusion is reinforced by the MgATP-hydrolysis rates, which are constant at 4.4 ± 0.2 ATP/2e$^-$ for both wild-type (α-277^{Arg}) and α-277^{His} in all four experiments. The data clearly show that N_2 neither binds to nor is reduced by the altered α-277^{His} MoFe protein.

Effect of Elevated Temperature on N_2 Reduction by the Altered α-277^{His} MoFe Protein. To test if temperature might affect the ability of the altered α-277^{His} MoFe protein to reduce N_2, assays were conducted at temperatures from 30 to 48 °C in approximately 5 °C increments using either wild-type (α-277^{Arg}) or α-277^{His} MoFe protein under either 100% Ar or 100% N_2. Both MoFe proteins approximately doubled their H_2-evolution activity in a linear manner as the temperature was increased from 30 to 48 °C when assayed under Ar. Under N_2, the α-277^{His} MoFe protein's response exactly duplicated its response under Ar with production of neither NH_3 nor N_2H_4. For wild-type, a linear increase in total flux was observed under N_2 to reach a maximum at 48 °C of 150% of the flux at 30 °C. As temperature was increased under N_2, the wild-type MoFe protein also preferentially evolved H_2, which accounted for about 35% of the electron flux at 30 °C and about 50% at 48 °C.

C_2H_2-Reduction Activity at High C_2H_2 Concentrations. To determine if higher concentrations of C_2H_2 would compete more effectively with protons for reduction catalyzed by the α-277^{His} MoFe protein, activity assays were conducted under high-flux conditions with concentrations of C_2H_2 ranging from 5 to 82% in Ar. The C_2H_2-reduction activities for both the wild-type and α-277^{His} MoFe proteins were maximal under about 20% C_2H_2, in agreement with previous studies of wild-type (Hwang & Burris, 1972), and accounted for 93 and 81% of electron flux, respectively. Thus, although higher C_2H_2 concentrations allow C_2H_2 to compete more effectively with protons, a consistently higher percentage of flux through the α-277^{His} MoFe protein was used for H_2 evolution throughout the C_2H_2 concentrations tested compared with wild-type as expected from its higher $K_m(C_2H_2)$. Over the range 20−82% C_2H_2, both C_2H_4 and H_2 production decreased gradually for both MoFe proteins, resulting in an overall decrease of ca. 30% in total electron flux at 82% C_2H_2 compared with 0% C_2H_2.

CO-Inhibition of C_2H_2-Reduction Activity at High and Low Electron Flux. When 10% CO was added to a high-flux assay under a 10% C_2H_2/90% Ar atmosphere, C_2H_4 formation ceased and the only observable product was H_2 with the flux through either the wild-type (α-277^{Arg}) or the α-277^{His} MoFe protein remaining effectively unchanged. When only 200 ppm CO was added to partially inhibit the reduction of C_2H_2, the two proteins responded differently. The wild-type MoFe protein displayed a normal hyperbolic response in Michaelis−Menten plots (Figure 3), which produced linear Lineweaver−Burk plots. In contrast, the production of C_2H_4 catalyzed by the α-277^{His} MoFe protein responded sigmoidally as a function of the C_2H_2 concentration (Figure 4) and produced upwardly curved Lineweaver−Burk plots, which approach a limiting horizontal line intersecting the $1/v$ axis at $1/V_{max}$. This result is consistent with the classic model of cooperativity (Segal, 1975). From a Hill plot, the estimated $n = 1.6$ indicates at least two ethylene-evolving sites on the enzyme and, as expected, plots of $1/v$ vs $1/[S]^2$ were linear. The same plot showed that, in the absence of CO, $1/v$ was not a linear function of $1/[S]^2$, indicating no cooperativity without CO. Thus, C_2H_4 production catalyzed by the altered α-277^{His} MoFe protein exhibits inhibitor-induced cooperativity among at least two C_2H_4-evolving sites.

To determine if this phenomenon was flux-related, a series of assays were performed under the more flux-limiting 4:1, 2:1, and 1:1 molar stoichiometries of Fe protein:MoFe protein. These assays showed both the expected decrease in overall substrate-reduction rates and the smaller percentage of flux going to reduce C_2H_2 for both wild-type and α-277^{His} MoFe proteins (data not shown) as the ratio decreased. However, the CO-induced cooperativity in C_2H_4 production catalyzed by the α-277^{His} MoFe protein remained under these low-flux conditions with Hill coefficients of approximately 1.4.

For the wild-type (α-277^{Arg}) MoFe protein assayed under maximal flux conditions, a K_m of 0.005 atm C_2H_2 and a V_{max}

Table 3: Kinetic Parameters for the Purified MoFe Proteins from DJ527 (α-277^{Arg}) and DJ788 (α-277^{His}) for a Variety of Alternative Substrates

substrate/ product	DJ527 (α-277^{Arg}) MoFe protein		DJ788 (α-277^{His}) MoFe protein	
	V_{max}[a]	K_m	V_{max}	K_m
C_2H_2/C_2H_4	1770	0.005 atm C_2H_2	870	0.051 atm C_2H_2
H^+/H_2	2400		982	
HCN/CH_4	135	2.6 mM[b] HCN	119	1.1 mM[b] HCN
HN_3/N_2H_4	158	7.1 μM[b] HN_3	113	24.2 μM[b] HN_3

[a] One unit of specific activity equals 1 nmol of product formed per minute per milligram of total protein in each assay, which contained a saturating amount of purified wild-type Fe protein. [b] The concentration of either HCN or HN_3 in solution at pH 7.4 was calculated from the NaCN or NaN_3 concentration, respectively, as described in the Experimental Procedures section.

of 1770 nmol of C_2H_4 (min mg)$^{-1}$ were calculated, plus a K_i of 0.000 15 atm CO for inhibition of C_2H_2 reduction, using the Fig.P program (Biosoft, Ferguson, MO). These values fall within the range reported previously (Hwang & Burris, 1972; Hwang *et al.*, 1973; Kim *et al.*, 1995). For the α-277^{His} MoFe protein, a K_m of 0.051 atm of C_2H_2 and a V_{max} of 870 nmol of C_2H_4 (min mg)$^{-1}$ were obtained using the same method, together with a K_i for CO inhibition of C_2H_2 reduction of 0.000 14 atm (Table 3). Thus, the higher K_m for C_2H_2 reduction by the α-277^{His} MoFe protein suggests a lower affinity for C_2H_2, whereas the same K_i for CO inhibition of C_2H_2 reduction suggests that the introduced amino-acid substitution has no effect on the affinity for CO.

Azide and Cyanide Reduction and CO Effects. The catalyzed reduction of the nitrogenase substrates present in pH-adjusted solutions of either sodium azide or sodium cyanide, with and without CO, was probed with the altered α-277^{His} MoFe protein as a comparison to the C_2H_2-reduction studies. Previous studies under intermediate flux conditions (Li *et al.*, 1982) have shown that, in a solution of NaCN, HCN is the Mo-nitrogenase substrate (K_m = 4.5 mM) whereas CN^- is a potent inhibitor (K_i = 27 μM) of total electron flux. Using aliquots of a 100-mM stock solution of NaCN under Ar at pH 7.4 in a high-flux assay, we determined a K_m of 2.6 mM HCN and a V_{max} of 135 nmol of CH_4 (min mg)$^{-1}$ for wild-type MoFe protein and a K_m of 1.1 mM HCN and a V_{max} of 119 nmol of CH_4 (min mg)$^{-1}$ for the α-277^{His} MoFe protein (Table 3). CO behaves as a noncompetitive inhibitor of catalyzed CH_4 formation from HCN by both wild-type and α-277^{His} MoFe proteins with no sigmoidal response and, therefore, without cooperativity. With assays using NaN_3 as a source of HN_3 and measuring N_2H_4 production, we calculated a K_m of 7.1 μM HN_3, which compares reasonably well with the published value (12 μM; Rubinson *et al.*, 1985), for wild-type (α-277^{Arg}) MoFe protein and a K_m of 24.2 μM HN_3 for the α-277^{His} MoFe protein (Tables 3 and 4). No sigmoidal response was observed either when CO was incorporated into these assays, where it behaved as a noncompetitive inhibitor of HN_3 reduction, or when C_2H_2 was used as an inhibitor of HN_3 reduction in an attempt to simulate the effect of CO on C_2H_2 reduction (data not shown). CO inhibits all substrate-reduction activities, except proton reduction, for both proteins. These data are summarized in Table 4.

DISCUSSION

The original design of our amino-acid substitution strategies, which were aimed at probing the polypeptide environment of FeMo cofactor, predated the availability of three-dimensional structural information (Brigle *et al.*, 1987a; Dean *et al.*, 1988). In these early studies, the strictly conserved α-arginine-277 residue was targeted as being located within the FeMo-cofactor-binding environment for several reasons. First, it is a near neighbor of the α-cysteine-275 residue, which was proposed to provide the mercaptide ligand that anchors FeMo cofactor to the MoFe-protein α-subunit (Brigle *et al.*, 1985; Kent *et al.*, 1989). Second, the potential importance of the α-arginine-277 was recognized through primary sequence comparisons with the *nifE* gene product, which, together with the *nifN* gene product, forms a molecular scaffold upon which FeMo cofactor is at least partially assembled (Brigle *et al.*, 1987b; Roll *et al.*, 1995). Finally, because the α-arginine-277 residue is positively charged and located in the FeMo cofactor-binding domain, it has been proposed as a potential candidate for accepting the negatively charged FeMo-cofactor during maturation of the MoFe protein (Scott *et al.*, 1992; Kim & Rees, 1992b). Figure 1 illustrates the relationship of α-arginine-277 to other residues located in the vicinity of FeMo cofactor and highlights its part in the surrounding hydrogen-bonding network. Inspection of the structural model shows that the α-arginine-277 residue appears appropriately positioned to impact both the orientation and functioning of FeMo cofactor within its polypeptide pocket, even though it is neither covalently bonded nor hydrogen bonded to FeMo cofactor. This possibility was confirmed in the present study where it is shown that all substitutions placed at the α-277 position variously alter the catalytic properties and spectroscopic features of the MoFe protein and provide insights into the nature of both the maturation and functioning of the MoFe protein. These insights are summarized below.

A Positively Charged Residue at α-277 Is Not Required for FeMo-cofactor Insertion. FeMo cofactor is separately synthesized and inserted into an apo-form of the MoFe protein (Ugalde *et al.*, 1984). The insertion of FeMo cofactor causes a conformational change, which is manifested by a change in electrophoretic mobility upon maturation (Govezensky & Zamir, 1989; Sal *et al.*, 1991; White *et al.*, 1992) and in the protection of the α-cysteine-275 residue from alkylating agents [cited in Peters *et al.* (1995b)]. Positively charged amino acids located within the FeMo-cofactor environment, for example, α-arginine-277, α-arginine-96, and α-arginine-359, are all likely candidates to be involved both in accepting the negatively charged FeMo cofactor and in eliciting the conformational change associated with FeMo-cofactor insertion. However, because both neutral and acidic amino acids can be placed at the α-277 position without dramatically changing the ability of the apo-MoFe protein to accept FeMo cofactor, arginine at this position is unlikely to have an important functional role in the maturation process. Those amino-acid substitutions that do have a dramatic effect on catalytic activity and also prevent insertion of the FeMo cofactor, *e.g.*, α-proline-277 and α-glycine-277, most likely elicit global effects rather than a specific effect on the ability to accept FeMo cofactor. In this context, the ability of the other altered MoFe proteins to accept FeMo cofactor is a good indication

Table 4: Substrates, Products, and Electron Distributions for the Wild-Type and α-277^{His} MoFe Proteins

		wild-type MoFe protein		α-277^{His} MoFe protein	
substrate	product[a]	SA[b]	SA (+ CO)[c]	SA	SA (+ CO)
10% C_2H_2	C_2H_4	1760 (87%)[d]	767 (35%)	543 (68%)	202 (24%)
	H_2	266 (13%)	1396 (65%)	259 (32%)	652 (76%)
H^+/100% Ar	H_2	2230 (100%)	2330 (100%)	1070 (100%)	1200 (100%)
100% N_2	H_2	701	1870	1060	1120
15.8 μM HN_3[e]	N_2H_4	112	78	35	9
	H_2	584	973	597	852
9.8 mM HCN[e]	CH_4	105	55	111	28
	H_2	304	1070	119	573

[a] All products were quantified for assays under 10% C_2H_2 and 100% Ar. Only the selected products shown were quantified using N_2, HCN, and HN_3 as substrates. [b] SA denotes the maximum specific activity of the appropriate MoFe protein, where 1 unit of activity equals 1 nmol of product formed/min mg of MoFe protein in the presence of saturating levels of wild-type Fe protein. All assays were performed in 25 mM Hepes-KOH buffer at pH 7.4 and 30 °C. [c] The CO concentration used in all assays was 0.06% except for those with HCN, when 0.025% CO was used. These concentrations were selected to partially inhibit catalyzed substrate reduction in order to visualize any unusual kinetic response. [d] Numbers in parentheses represent the percentage of total electron flux to each product. [e] These concentrations of HN_3 and HCN were calculated as being present at a pH of 7.4 in 10 mM NaN_3 and NaCN solutions, respectively (see Experimental Procedures).

that their changed catalytic and spectroscopic features are most likely the result of a relatively minor perturbation within the local FeMo-cofactor environment rather than from gross structural changes. This assertion is further supported by the similarity of the major signals in their whole-cell EPR spectra to those of wild-type.

Are Multiple Redox States Involved in Substrate Binding and Reduction? The Lowe−Thorneley model of Mo-nitrogenase turnover (Lowe & Thorneley, 1984) proposes that N_2 binds to the more-reduced E_3 or E_4 level (after accepting three or four electrons, respectively) of the MoFe protein whereas the alternative substrates bind to the less-reduced E_1 and E_2 levels (after accepting one or two electrons, respectively). Our observation that the α-277^{His} MoFe protein is unable to bind N_2, while still being able to bind and reduce C_2H_2, HN_3, HCN, and H^+, is most easily explained if the less-reduced E_1 and E_2 levels are well populated in the α-277^{His} MoFe protein whereas the more-reduced E_3 and E_4 levels are unattainable. This situation can be compared to low-flux conditions for wild-type catalysis, where the apparent K_m for N_2 reduction increases relative to high-flux conditions and protons become preferentially reduced (Davis *et al.*, 1975; Wherland *et al.*, 1981). Previously, it was found (Dilworth & Thorneley, 1981) with the *Klebsiella pneumoniae* enzyme that N_2 acts as a competitive inhibitor of the six-electron reduction of HN_3 to yield N_2H_4, yet the K_i for N_2 as an inhibitor of this reaction is 10-times larger than the K_m for N_2 reduction to NH_3. This result is also explainable by the Lowe−Thorneley model, where the same binding site is used for both N_2 and HN_3 reduction but each substrate binds at a different redox level. In line with this reasoning, the substitution of α-arginine-277 by histidine appears not to disturb dramatically the physical nature of this substrate-binding site because the altered MoFe protein remains able to reduce HN_3 effectively with an apparent affinity for this alternative substrate that is only about 2−3 times less than wild-type.

In addition, it might be that the required conditions for N_2 binding and reduction are never achieved because the substitution physically changes the nature of the substrate-reduction site, such that H_2 evolution becomes greatly favored. Direct evidence for an alteration in the substrate-reducing site within the α-277^{His} MoFe protein is provided by a comparison of its measured K_m for C_2H_2, HN_3, and HCN reduction with those of wild-type. For C_2H_2 and HN_3, the K_m is increased for the altered MoFe protein, whereas the K_m for HCN reduction is decreased. These differential effects cannot be explained by the enzyme's inability to achieve a particular redox level. Rather, it is more likely that a subtle, substitution-induced change in the FeMo-cofactor environment has placed different constraints on either binding or reduction of each of these alternative substrates. These observations suggest that the polypeptide environment of FeMo cofactor plays an important role in controlling substrate binding and reduction such that N_2 binding and reduction are normally favored under physiological conditions. Otherwise stated, the wild-type nitrogenase might gate the production of H_2 so that the proper redox level for N_2 binding is attained and reduction to NH_3 is achieved. Therefore, both the inability of the α-277^{His} MoFe protein to achieve the redox level necessary to bind N_2 and its uncontrolled H_2 production could be due to the loss of this gating mechanism as a consequence of the histidine-for-arginine substitution. The observation that the α-277^{His} MoFe protein allocates a relatively higher percentage of electron flux to H_2 evolution than does wild-type, even under C_2H_2-reduction conditions, supports this possibility.

CO-Induced Cooperativity of C_2H_2 Reduction Catalyzed by the Altered α-277^{His} MoFe Protein Provides Evidence for Multiple Substrate-Binding Sites. As found for wild-type Mo-nitrogenase, α-277^{His} MoFe-protein-catalyzed C_2H_2 reduction is inhibited noncompetitively by CO. Also, like wild-type, at nonsaturating CO levels when only partial inhibition of catalyzed C_2H_2 reduction occurs, the loss of C_2H_4 production is compensated by an elevated H_2-evolution activity, such that total electron flux remains constant. In addition, however, C_2H_2 reduction catalyzed by the α-277^{His} MoFe protein in the presence of nonsaturating amounts of CO exhibits sigmoidal kinetics, which indicate cooperativity among at least two sites for C_2H_4 production. Previous studies of C_2H_2 reduction and its inhibition by CO have raised the possibility of multiple sites for both C_2H_2 and CO on nitrogenase. Substrate self-inhibition at high C_2H_2 concentrations (Hwang & Burris, 1972), shown by both wild-type and α-277^{His} MoFe proteins, suggests the presence of an additional lower-affinity site(s) for C_2H_2 binding. But, as occupancy of this site normally requires high C_2H_2 concentrations and leads to inhibition, it is unlikely to be involved in the observed cooperativity. Further, two popula-

tions, a low K_m(for C_2H_2) form and a high K_m(for C_2H_2) form, have been suggested to exist in wild-type nitrogenase preparations (Davis *et al.*, 1979). Rather than indicating different populations, these two K_m's could reflect two noninteracting sites on the same enzyme molecule. We prefer this second interpretation, which is consistent with our data.

Because the two FeMo-cofactor prosthetic groups within the MoFe-protein $\alpha_2\beta_2$ tetramer are 70 Å apart and the α-subunits within which they are bound are "insulated" from each other by the intervening β-subunits (Kim & Rees, 1992a,b), we believe it very unlikely that the observed cooperativity is due to the classical Monod mechanism of induced α-subunit conformational changes (Monod *et al.*, 1965). For the same reason, it is unattractive to correlate the two individual "forms" of FeMo cofactor, presumably present and responsible for the two $S = 3/2$ EPR signals exhibited by the resting state of the MoFe protein, with the two C_2H_4-evolving sites because it is difficult to visualize how binding CO could induce cooperativity in this situation. It is also unlikely that two different redox levels of the MoFe protein (and, therefore, of FeMo cofactor) are involved because the same result was obtained under both high- and low-flux conditions. More satisfying is a mechanism in which two sites for C_2H_4 evolution normally coexist in the vicinity of each FeMo cofactor and the potential for communication among them has been induced by the slight rearrangement of the polypeptide in the FeMo-cofactor environment. Communication is then effected by the binding of CO. In this model, each FeMo cofactor (E) within the enzyme forms the ternary complex, E(CO)−$(C_2H_2)_2$, which gives rise to product (C_2H_4) more rapidly than E(CO)−(C_2H_2). Implicit in this mechanism is the fact that the CO- and C_2H_2-binding sites are independent of each other, which is consistent with the known noncompetitive pattern of inhibition by CO of all substrate reductions [reviewed by Burgess (1985)]. In this context, it is worth noting that the K_m for C_2H_2 reduction is significantly increased by the α-histidine-277 substitution, whereas the substitution has no effect on the K_i for CO inhibition of C_2H_2 reduction, when compared with the wild-type parameters.

We also asked if CO-induced cooperativity extends to the reduction of either HN_3 or HCN catalyzed by the α-277^{His} MoFe protein. Like wild-type, saturating CO concentrations completely inhibited the reduction of both HN_3 and HCN catalyzed by the α-277^{His} MoFe protein. However, neither CH_4 production from HCN nor N_2H_4 production from HN_3 showed a sigmoidal response in the presence of partially inhibiting levels of CO, indicating that inhibitor-induced cooperativity does not occur for these substrates and suggesting either that these two alternative substrates have different structural constraints placed on their binding and/or reduction or that they bind at a site(s) distinct from the C_2H_2-binding sites. The fact that the K_m for HCN reduction catalyzed by the α-277^{His} MoFe protein decreases relative to wild-type, whereas the K_m for C_2H_2 reduction increases, argues in support of distinct reduction sites.

Because all substrates compete for the electron flux passing through the MoFe protein, a related question to be asked was whether the various chemical species in solutions of either NaN_3 or NaCN might induce cooperativity during their inhibition of C_2H_2 reduction. In this regard, we were particularly interested in the electron-flux inhibitor, CN^-, because, with wild-type, its potent inhibitory effect can be completely reversed by CO, suggesting the possibility of a common binding site for both CO and CN^- (Li *et al.*, 1982). However, no induced cooperativity in C_2H_4 production from C_2H_2 catalyzed by the altered α-277^{His} MoFe protein was observed when CN^- was present. We conclude that there is an unique interaction between CO binding and C_2H_4 evolution, which does not exist with any other substrate−inhibitor combination used. The exact nature of the relationship among the CO-binding site(s) and the two C_2H_4-evolution sites around each FeMo cofactor in the α-277^{His} MoFe protein remains unclear, although it is likely that, in order to interact, two (at least) of them are in close proximity to each other.

CONCLUSIONS

First, characterization of altered MoFe proteins having a variety of different substitutions at the α-arginine-277 residue position indicates that this residue is unlikely to have an important role in the insertion of FeMo cofactor into the immature apo-form of the MoFe protein.

Second, all of the information that we have gathered regarding the effects of substitution at the α-arginine-277 residue suggests that this residue is important in enzyme functioning. Together with results reported from the previous characterization of other altered MoFe proteins (Scott *et al.*, 1990, 1992; Kim *et al.*, 1995), it is clear that the FeMo cofactor's polypeptide environment is intimately involved in the delicate control of the MoFe protein's ability to bind and allocate electrons among substrates. Indeed, physiological control of the allocation of electron flux among proton reduction and N_2 reduction must be a vital aspect of the catalytic mechanism because H_2 evolution appears to be obligatorily coupled to N_2 binding and reduction (Simpson & Burris, 1984).

Third, the two C_2H_4-evolving sites, which were elicited by nonsaturating CO levels, on the α-277^{His} MoFe protein could be operational without bound CO present. Both sites may also be present on wild-type MoFe protein. In both instances, they would be indistinguishable from one another under the normal assay conditions. Further, because CO-induced cooperativity was not observed during HN_3 and HCN reduction catalyzed by the α-277^{His} MoFe protein, HN_3 and HCN either do not bind to more than one site or, if they do, their binding is not cooperative, which suggests that they may not share common binding and reduction sites with C_2H_2.

Fourth, the noncompetitive pattern of CO inhibition of all substrate reductions could be due to either CO binding to a different site than do the substrates or CO binding to the same site but at a different redox level. The CO-induced cooperativity observed for C_2H_2 reduction by α-277^{His} MoFe protein demonstrates that CO binds simultaneously with C_2H_2. Thus, CO binds to a different site on the MoFe protein but at the same redox level.

Fifth, it is unlikely that the inhibitors, CO and CN^-, share a common binding site on the MoFe protein because, unlike CO, CN^- did not induce cooperativity during C_2H_4 production from C_2H_2 catalyzed by the α-277^{His} MoFe protein. Any alternative explanation, which postulates an alteration in the CO-binding site due to the arginine-to-histidine substitution, appears untenable because the K_i for CO inhibition of C_2H_2

reduction is the same for both wild-type and the α-277^{His} MoFe protein.

Finally, all of our kinetic results, using a variety of different substrates and inhibitors, can be viewed in the context of the structural model for the FeMo cofactor. This model has six coordinatively unsaturated Fe atoms, each of which is surrounded by three sulfide ions in a nearly trigonal planar geometry. These low-coordination-number Fe atoms in close proximity to one another are likely candidates to either provide or participate in forming the multiple substrate- and inhibitor-binding sites revealed by the present work. Of particular relevance is that these six Fe atoms are arranged such that they are shared among three geometrically similar faces, whose accessibility and electronic properties may well be distinguished by the amino-acid side chains that approach and/or interact with them (see Figure 1). In this context, the α-381^{Phe} residue protrudes into one of these faces, the α-359^{Arg} residue spans a second face (providing a putative NH−S bond with a S coordinated to the Mo atom of FeMo cofactor), and α-96^{Arg} associates with the third face (also with putative NH−S bonding). From this perspective, it is easy to visualize different substrates and inhibitors occupying distinct, and, in some cases, overlapping sites and some recent theoretical treatments (Sellmann, 1993; Deng & Hoffmann, 1993; Dance, 1994; Stavrev & Zerner, 1996) of possible N_2-binding modes and N_2-binding sites highlight this possibility. The phenomenon of "overlap" in sites could occur either by a direct effect, which occurs through the participation of an individual metal or sulfur atom in more than one substrate/inhibitor-binding site, or by an indirect effect, which involves steric constraints that arise because the binding of substrate/inhibitor to one site affects (either restricts or enhances) the binding of substrate/inhibitor to a distinct, neighboring site. We suggest that such steric constraints are operational in the CO-induced cooperativity of C_2H_2 reduction observed in this work. A related example is provided by the α-195^{Gln} MoFe protein, which cannot reduce N_2 even though N_2 is a potent inhibitor of both proton and C_2H_2 reduction (Kim *et al.*, 1993). Such dramatic changes in kinetic properties and interactions among substrates and inhibitors, which arise as a consequence of amino-acid substitution within the FeMo-cofactor pocket, clearly indicate that some of the substrate/inhibitor-binding sites are located in rather close proximity to one another, consistent with the description of the FeMo-cofactor structural model discussed above. However, our results also show that certain types of these substrate/inhibitor-binding sites are capable of operating independently of each other. Thus, the studies reported here indicate that the nitrogenase MoFe protein should be viewed as a very versatile enzyme component, which is capable of presenting multiple substrate- and inhibitor-binding sites and assuming multiple redox levels.

ACKNOWLEDGMENT

We thank W. R. Dunham and R. H. Sands (University of Michigan) for assistance with EPR spectroscopy, V. Cash (Virginia Tech) for assistance with mutant construction, J. T. Rinehart (Virginia Tech) for the Mo and Fe analyses, and K. Fisher (Virginia Tech) and M. J. Dilworth (Murdoch University, W. Australia) for their expert advice and critical reading of the manuscript.

REFERENCES

Bolin, J. T., Campobasso, N., Muchmore, S. M., Minor, W., Morgan, T. V., & Mortenson, L. E. (1993a) in *New horizons in nitrogen fixation* (Palacios, R., Mora, J., & Newton, W. E., Eds.) pp 89−94, Kluwer Academic, Dordrecht, The Netherlands.

Bolin, J. T., Campobasso, N., Muchmore, S. M., Morgan, T. V., & Mortenson, L. E. (1993b) in *Molybodoenzymes, cofactors and model systems* (Stiefel, E. I., Coucouvanis, D., & Newton, W. E., Eds.) pp 186−195, American Chemical Society, Washington, DC.

Brigle, K. E., Newton, W. E., & Dean, D. R. (1985) *Gene 37*, 37−44.

Brigle, K. E., Setterquist, R. A., Dean, D. R., Cantwell, J. S., Weiss, M. C., & Newton, W. E. (1987a) *Proc. Natl. Acad. Sci. U.S.A. 84*, 7066−7069.

Brigle, K. E., Weiss, M. C., Newton, W. E., & Dean, D. R. (1987b) *J. Bacteriol. 169*, 1547−1553.

Bulen, W. A., Burns, R. C., LeComte, J. R., & Hinkson, J. (1965) in *Non-heme iron proteins: role in energy conversion* (San Pietro, A., Ed.) pp 261−274, Antioch Press, Yellow Springs, OH.

Burgess, B. K. (1985) in *Molybdenum enzymes* (Spiro, T., Ed.) pp 161−220, Wiley-Interscience, New York.

Burgess, B. K., Jacobs, D. J., & Stiefel, E. I. (1980) *Biochim. Biophys. Acta 614*, 196−209.

Burns, R. C., & Bulen, W. A. (1965) *Biochim. Biophys. Acta 105*, 437−445.

Chan, M. K., Kim, J., & Rees, D. C. (1993) *Science 260*, 792−794.

Corbin, J. L. (1978) *Anal. Biochem. 84*, 340−342.

Dance, I. G. (1994) *Aust. J. Chem. 47*, 979−990.

Davis, L. C., Shah, V. K., & Brill, W. J. (1975) *Biochim. Biophys. Acta 403*, 67−78.

Davis, L. C., Henzl, M. T., Burris, R. H., & Orme-Johnson, W. H. (1979) *Biochemistry 18*, 4860−4869.

Dean, D. R., Brigle, K. E., May, H. D., & Newton, W. E. (1988) in *Nitrogen Fixation: Hundred Years After* (Bothe, H., deBruijn, F. J., & Newton, W. E., Eds.) pp 107−113, Gustav Fischer, Stuttgart.

Dean, D. R., Setterquist, R. A., Brigle, K. E., Scott, D. J., Laird, N. F., & Newton, W. E. (1990) *Mol. Microbiol. 4*, 1505−1512.

Deng, H., & Hoffmann, R. (1993) *Angew. Chem., Int. Ed. Engl. 32*, 1062−1065.

DeRose, V. J., Kim, C.-H., Newton, W. E., Dean, D. R., & Hoffman, B. M. (1995) *Biochemistry 34*, 2809−2814.

Dilworth, M. J. (1966) *Biochim. Biophys. Acta 127*, 285−294.

Dilworth, M. J., & Thorneley, R. N. F. (1981) *Biochem. J. 193*, 971−983.

Dilworth, M. J., Eldridge, M. E., & Eady, R. R. (1992) *Anal. Biochem. 206*, 6−10.

Govezensky, D., & Zamir, A. (1989) *J. Bacteriol. 171*, 5729−5735.

Hageman, R. V., & Burris, R. H. (1978) *Proc. Natl. Acad. Sci. U.S.A. 75*, 2699−2702.

Hardy, R. W. F., Knight, E., Jr., & D'Eustachio, A. J. (1965) *Biochem. Biophys. Res. Commun. 20*, 539−544.

Hawkes, T. R., McLean, P. A., & Smith, B. E. (1984) *Biochem. J. 217*, 317−321.

Hwang, J. C., & Burris, R. H. (1972) *Biochim. Biophys. Acta 283*, 339−350.

Hwang, J. C., Chen, C. H., & Burris, R. H. (1973) *Biochim. Biophys. Acta 292*, 256−270.

Jacobson, M. R., Cash, V. L., Weiss, M. C., Laird, N. F., Newton, W. E., & Dean, D. R. (1989) *Mol. Gen. Genet. 219*, 49−57.

Kent, H. M., Ioannidis, I., Gormal. C., Smith, B. E., & Buck, M. (1989) *Biochem. J. 264*, 257−264.

Kim, C.-H., Zheng, L., Newton, W. E., & Dean, D. R. (1993) in *New horizons in nitrogen fixation* (Palacios, R., Mora, J., & Newton, W. E., Eds.) pp 105−110, Kluwer Academic, Dordrecht, The Netherlands.

Kim, C.-H., Newton, W. E., & Dean, D. R. (1995) *Biochemistry 34*, 2798−2808.

Kim, J., & Rees, D. C. (1992a) *Science 257*, 1677−1682.

Kim, J., & Rees, D. C. (1992b) *Nature 360*, 553−560.

Kim, J., & Rees, D. C. (1994) *Biochemistry 33*, 389−397.

Kraulis, P. (1991) *J. Appl. Crystallogr. 24*, 946−950.

Laemmli, U. K. (1970) *Nature 227*, 680−685.
Li, J.-G., Burgess, B. K., & Corbin, J. L. (1982) *Biochemistry 21*, 4393−4402.
Lowe, D. J., & Thorneley, R. N. F. (1984) *Biochem. J. 224*, 886−909.
Lowe, D. J., Fisher, K., & Thorneley, R. N. F. (1990) *Biochem. J. 272*, 621−625.
Lowe, D. J., Fisher, K., & Thorneley, R. N. F. (1993) *Biochem. J. 292*, 93−98.
Monod, J., Wyman, J., & Changeux, J.-P. (1965) *J. Mol. Biol. 12*, 88−95.
Newton, W. E., & Dean, D. R. (1993) in *Molybodoenzymes, cofactors and model systems* (Stiefel, E. I., Coucouvanis, D., & Newton, W. E., Eds.) pp 216−230, American Chemical Society, Washington, DC.
Peters, J. W., Fisher, K., Newton, W. E., & Dean, D. R. (1995a) *J. Biol. Chem. 270*, 27007−27013.
Peters, J. W., Fisher, K., & Dean, D. R. (1995b) *Annu. Rev. Microbiol. 49*, 335−366.
Rivera-Ortiz, J. M., & Burris, R. H. (1975) *J. Bacteriol. 123*, 537−545.
Roll, J. T., Shah, V. K., Dean, D. R., & Roberts, G. P. (1995) *J. Biol. Chem. 270*, 4432−4437.
Rubinson, J. F., Burgess, B. K., Corbin, J. L., & Dilworth, M. J. (1985) *Biochemistry 24*, 273−283.
Sal, S., Chun, W., Gavini, N., & Burgess, B. K. (1991) *J. Biol. Chem. 266*, 10654−10657.
Scott, D. J., May, H. D., Newton, W. E., Brigle, K. E., & Dean, D. R. (1990) *Nature 343*, 188−190.
Scott, D. J., Dean, D. R., & Newton, W. E. (1992) *J. Biol. Chem. 267*, 20002−20010.
Segal, I. H. (1975) *Enzyme kinetics: Behavior and analysis of rapid equilibrium and steady-state systems*, John Wiley & Sons, New York.
Sellmann, D. (1993) *Angew. Chem., Int. Ed. Engl. 32*, 64−67.
Shah, V. K., & Brill, W. J. (1977) *Proc. Natl. Acad. Sci. U.S.A. 74*, 3249−3253.
Silverstein, R., & Bulen, W. A. (1970) *Biochemistry 9*, 3809−3815.
Simpson, F. B., & Burris, R. H. (1984) *Science 224*, 1095−1097.
Smith, P. K., Krohn, R. I., Hermanson, G. T., Mallia, A. K., Gartner, F. H., Provenzano, M. D., Fujimoto, E. K., Goeke, N. M., Olson, B. J., & Klenk, D. C. (1985) *Anal. Biochem. 150*, 76−85.
Stavrev, K. K., & Zerner, M. C. (1996) *Chem. Eur. J. 2*, 83−87.
Strandberg, G. W., & Wilson, P. W. (1968) *Can. J. Microbiol. 14*, 25−31.
Thorneley, R. N. F., Eady, R. R., & Lowe, D. J. (1978) *Nature 272*, 557−558.
Ugalde, R. A., Imperial, J., Shah, V. K., & Brill, W. J. (1984) *J. Bacteriol. 164*, 1081−1087.
White, T. C., Harris, G. S., & Orme-Johnson, W. H. (1992) *J. Biol. Chem. 164*, 24007−24016.
Wherland, S., Burgess, B. K., Stiefel, E. I., & Newton, W. E. (1981) *Biochemistry 20*, 5132−5140.

BI9628578